

## **Compact Environmental Anomaly Sensor (CEASE) Flight Integration Support Contract**

<b>Robert H. Redus</b>	<b>Bronislaw K. Dichter</b>	<b>Marilyn R. Oberhardt</b>
<b>John O. McGarity</b>	<b>David J. Sperry</b>	<b>Scott J. Moran</b>
<b>Valentin T. Jordanov</b>	<b>Phillip G. D'Entremont</b>	<b>John A. Pantazis</b>
<b>Alan C. Huber</b>	<b>Thanos Pantazis</b>	

**AMPTEK, Inc.  
6 DeAngelo Drive  
Bedford, MA 01730**

**26 November 2001**

**Final Report**

**20020305 075**

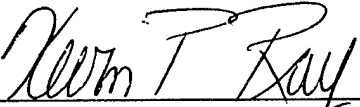
**APPROVED FOR PUBLIC RELEASE; DISTRIBUTION IS UNLIMITED.**



**AIR FORCE RESEARCH LABORATORY  
Space Vehicles Directorate  
29 Randolph Rd  
AIR FORCE MATERIEL COMMAND  
Hanscom AFB, MA 01731-3010**

---

“ This technical report has been reviewed and is approved for publication.”

  
\_\_\_\_\_  
KEVIN P. RAY  
Contract Manager

  
\_\_\_\_\_  
CARL J. CHRISTENSEN, Maj, USAF  
Acting Chief, SWx Center of Excellence

This report has been reviewed by the ESC Public Affairs Office (PA) and is releasable to the National Technical Information Service (NTIS).

Qualified requestors may obtain additional copies from the Defense Technical Information Center (DTIC). All others should apply to the National Technical Information Service (NTIS).

If your address has changed, if you wish to be removed from the mailing list, or if the addressee is no longer employed by your organization, please notify PL/IM, 29 Randolph Road, Hanscom AFB, MA. 01731-3010. This will assist us in maintaining a current mailing list.

Do not return copies of this report unless contractual obligations or notices on a specific document require that it be returned.

**REPORT DOCUMENTATION PAGE**

*Form Approved  
OMB No. 0704-0188*

The public reporting burden for this collection of information is estimated to average 1 hour per response, including the time for reviewing instructions, searching existing data sources, gathering and maintaining the data needed, and completing and reviewing the collection of information. Send comments regarding this burden estimate or any other aspect of this collection of information, including suggestions for reducing the burden, to Department of Defense, Washington Headquarters Services, Directorate for Information Operations and Reports (0704-0188), 1215 Jefferson Davis Highway, Suite 1204, Arlington, VA 22202-4302. Respondents should be aware that notwithstanding any other provision of law, no person shall be subject to any penalty for failing to comply with a collection of information if it does not display a currently valid OMB control number.  
**PLEASE DO NOT RETURN YOUR FORM TO THE ABOVE ADDRESS.**

<b>1. REPORT DATE (DD-MM-YYYY)</b> 26-11-2001		<b>2. REPORT TYPE</b> Final		<b>3. DATES COVERED (From - To)</b> 15 April 1996 - 01 January 2001	
<b>4. TITLE AND SUBTITLE</b> COMPACT ENVIRONMENTAL ANOMALY SENSOR (CEASE) FLIGHT INTEGRATION SUPPORT				<b>5a. CONTRACT NUMBER</b> F19628-96-C-0063	
				<b>5b. GRANT NUMBER</b>	
				<b>5c. PROGRAM ELEMENT NUMBER</b> 63401F	
<b>6. AUTHOR(S)</b> Robert H. Redus, Bronislaw K. Dichter, Marilyn R. Oberhardt, John O. McGarity, David J. Sperry, Scott J. Moran, Valentin T. Jordanov, Phillip G. d'Entremont, John A. Pantazis, Alan C. Huber, and Thanos Pantazis				<b>5d. PROJECT NUMBER</b> 2823	
				<b>5e. TASK NUMBER</b> GC	
				<b>5f. WORK UNIT NUMBER</b> CE	
<b>7. PERFORMING ORGANIZATION NAME(S) AND ADDRESS(ES)</b> Amptek Inc. 6 DeAngelo Drive Bedford, MA. 01730				<b>8. PERFORMING ORGANIZATION REPORT NUMBER</b>	
<b>9. SPONSORING/MONITORING AGENCY NAME(S) AND ADDRESS(ES)</b> Air Force Research Laboratory/Space Vehicles Directorate 29 Randolph Rd. Hanscom AFB, MA 01731-3010				<b>10. SPONSOR/MONITOR'S ACRONYM(S)</b> AFRL/VSBS	
				<b>11. SPONSOR/MONITOR'S REPORT NUMBER(S)</b> AFRL-VS-TR-2001-1601	
<b>12. DISTRIBUTION/AVAILABILITY STATEMENT</b> Approved for public Release; Distribution unlimited.					
<b>13. SUPPLEMENTARY NOTES</b> Contract Manager Kevin Ray/VSBS					
<b>14. ABSTRACT</b> This document is the Final Report for the Compact Environmental Anomaly Sensor (CEASE) Flight Support Program carried out by Amptek, Inc. under Air Force contract F19628-96-C-0063. The goal of this program was to support the flight code development, functional testing, environmental testing, calibration spacecraft integration, and initial on-orbit checkout of the CEASE S/N 001 and S/N 002 instruments. These instruments were built by Amptek, Inc. under the Air Force contract F19628-90-C-0159. The basic instrument descriptions can be found in the final report for the previous contract. Under the current contract, Amptek Inc, supported the successful spacecraft specific design work, final calibration, and the delivery, integration, and launch of two CEASE instruments - S/N 001 onto the Space Test Research Vehicle 1c (STRV-1c) spacecraft and S/N 002 onto the Tri-Service Experiment 5 (TSX-5) spacecraft. This report documents the work conducted by Amptek on these CEASE flight units and an accompanying engineering unit, under the current contract.					
<b>15. SUBJECT TERMS</b> CEASE, space radiation, environmental anomaly sensor, surface dielectric charging, deep dielectric charging, single event effects, ionizing radiation dose, space weather warnings.					
<b>16. SECURITY CLASSIFICATION OF:</b>			<b>17. LIMITATION OF ABSTRACT</b> UU	<b>18. NUMBER OF PAGES</b>	<b>19a. NAME OF RESPONSIBLE PERSON</b> Kevin Ray
<b>a. REPORT</b> U	<b>b. ABSTRACT</b> U	<b>c. THIS PAGE</b> U			<b>19b. TELEPHONE NUMBER (Include area code)</b> 781-377-3828

## Table of Contents

1	Summary .....	1
2	CEASE Instrument description .....	1
2.1	Measured Threats .....	3
2.1.1	Radiation Dose.....	3
2.1.2	Single Event Effects .....	3
2.1.3	Spacecraft Charging .....	3
2.1.4	On-board Processing .....	4
2.2	Hazard Registers and Warning Flags .....	5
2.3	Operating CEASE .....	6
3	Sensor Response: Models, Tests, and Calibration .....	7
3.1	Dosimeters .....	7
3.2	Telescope.....	8
3.3	SEE Sensor.....	12
4	Flight Software.....	13
4.1	Status Register Algorithms.....	13
4.2	Conversion to Engineering Units.....	16
4.3	Rationale For Charging Algorithms .....	16
4.3.1	Surface Charging .....	17
4.3.2	Electron Flux Provides Advance Warning.....	18
4.3.3	Deep Dielectric Charging .....	18
5	Spacecraft Specific Design, fabrication, and Test.....	20
5.1	Spacecraft Specific Hardware .....	20
5.2	Flight Software .....	20
5.3	GSE Software.....	21
5.4	Environmental Testing.....	23
5.5	Integration and Launch Support Activities.....	23

## 1 SUMMARY

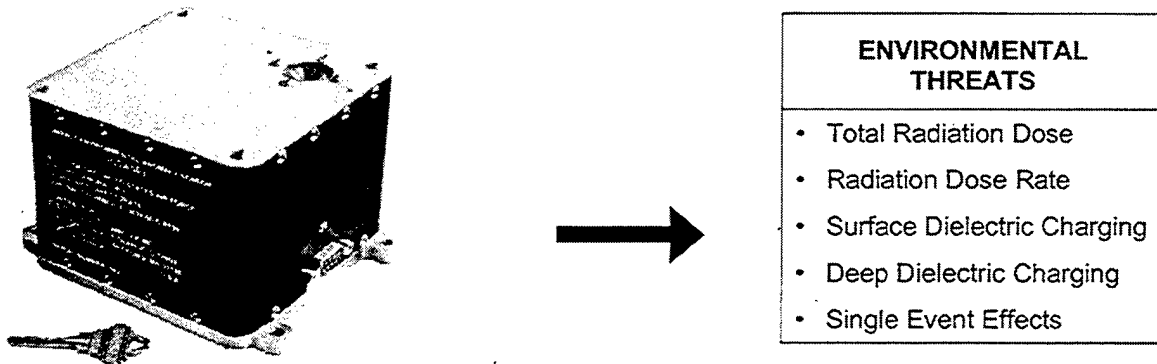
This document is the Final Report for the Compact Environmental Anomaly Sensor (CEASE) Flight Support Program carried out by Amptek, Inc. under the Air Force contract F19628-96-C-0063. The goal of this program was to support the flight code development, functional testing, environmental testing, calibration spacecraft integration, and initial on-orbit checkout of the CEASE S/N 001 and S/N 002 instruments. These instruments were built by Amptek, Inc. for AFRL/VSBS under the Air Force contract F19628-90-C-0159. The basic instrument descriptions can be found in the final report for the previous contact, and in a published research paper:

Dichter, B.K, J. O. McGarity, M. R. Oberhardt, V. T. Jordanov, D. J. Sperry, A. C. Huber, J. A. Pantazis, E. G. Mullen, G. Ginet and M. S. Gussenhoven, "Compact Environmental Anomaly Sensor (CEASE): A Novel Spacecraft Instrument for In-Situ Measurement of Environmental Conditions", *IEEE Trans. Nucl. Sci.*, Vol 45, No. 6, p. 2758, December 1998.

Under the current contract, Amptek Inc, supported the successful spacecraft specific design work, final calibration, and the delivery, integration, and launch of two CEASE instruments – S/N 001 onto the Space Test Research Vehicle 1c (STRV-1c) spacecraft and S/N 002 onto the Tri-Service Experiment 5 (TSX-5) spacecraft. This report documents the work conducted by Amptek on these CEASE flight units and an accompanying engineering unit, under the current contract.

## 2 CEASE INSTRUMENT DESCRIPTION

Today's space systems demand high performance and reliability. However, satellites operate in a hostile environment, bombarded by ionizing radiation from a variety of natural sources. Ionizing radiation damages electronic components and systems, with consequences ranging from minor performance degradation to catastrophic system failure. Cost effective and simple ways to reduce this risk both in the design and operation of the spacecraft are needed. The solution is a multipurpose easily integrated, environmental hazard sensor package, the Compact Environmental Anomaly Sensor (CEASE).



Spacecraft operators must prevent degradation in performance and failure of space-borne systems. With real-time warnings that the environment is likely to cause anomalies, operators can alter spacecraft operations to minimize risk to their systems. Today, space "weather" forecasts serve as these warnings. But the forecasts do not provide the real-time local conditions required for operators to take corrective action.

Anomalies or failures do occur, and the tools to understand their causes are needed. Space environmental effects must be isolated from other causes of system failures. When operators have to pinpoint the definitive cause of a spacecraft anomaly, real-time, *in situ* monitoring is needed. Without it, time, money and even satellites are lost. With such monitoring, operators can modify operations during hazardous conditions, predict performance loss and end of life, and launch replacement satellites if necessary.

CEASE is a small, low power instrument that provides operators with fully processed, real time, *in situ* measurements and autonomously generated warnings of the space radiation environment threats. CEASE reports these threats to the host spacecraft:

- Ionizing radiation dose and dose rates
- Single event effects
- Surface and deep dielectric charging

The primary CEASE output to the spacecraft, updated once per minute, is a 10-byte *Engineering Data* packet quantifying the threat levels associated with those space environment hazards. Appropriate action may then be taken by the spacecraft or its operators to mitigate risk. The CEASE hazard registers are described in Table 2.

With its suite of sensors and sophisticated onboard data processing, CEASE is an extremely flexible stand-alone diagnostic instrument. CEASE is a solution to the problem of space environmental monitoring for both operational and experimental spacecraft. There are two versions of CEASE available to provide the necessary monitoring. CEASE II includes an additional sensor to better characterize the surface charging in geosynchronous orbits. Table 1 summarizes the general properties of the two instruments.

Table 1. Summary of CEASE Properties

	CEASE I	CEASE II
Size	4.0 x 4.0 x 3.2 "	5.0 x 5.1 x 3.2 "
Mass	1.0 kg	1.3 kg
Power <sup>1</sup>	1.5 Watts	1.7 Watts
Telemetry (minimum)	10 bytes per 60 sec	10 bytes per 60 sec
Diagnostic Sensors	Lightly Shielded Dosimeter Heavily Shielded Dosimeter SEE Detector Particle Telescope	Lightly Shielded Dosimeter Heavily Shielded Dosimeter SEE Detector Particle Telescope Electrostatic Analyzer

Table 2. CEASE Hazard Registers

Name	Acronym	Description	Typical Dynamic Range
Lightly Shielded Dose	LSD	Mission integrated radiation dose behind 0.08 inches of Al	0.2 to 118 krad
Heavily Shielded Dose	HSD	Mission integrated radiation dose behind 0.25 inches of Al	0.1 to 59 krad
Lightly Shielded Dose Rate	LSR	Radiation dose rate over the last minute behind 0.08 inches of Al	0.04 to 27 rads/hr
Heavily Shielded Dose Rate	HSR	Radiation dose rate over the last minute behind 0.25 inches of Al	0.04 to 27 rads/hr
Surface Dose	SUD	Solar panel damage parameter: "effective 1 MeV electron fluence"	$1.8 \times 10^{13}$ to $5.6 \times 10^{16}$ electrons/cm <sup>2</sup>
Single Event Effect	SEE	Register value is proportional to SEE probability	0 to 255 (linear)
Surface Dielectric Charging	SDC	Electron flux responsible for surface dielectric charging (50 < E < 250 keV)	$5.0 \times 10^4$ to $2.3 \times 10^9$ electrons/cm <sup>2</sup> -sec
Deep Dielectric Charging	DDC	Electron flux responsible for deep dielectric charging (E > 250 keV)	$4.2 \times 10^3$ to $1.9 \times 10^8$ electrons/cm <sup>2</sup> -sec

<sup>1</sup> Measured with RS422 interface. Power requirements will vary for other interfaces.

## 2.1 MEASURED THREATS

CEASE measures the environmental hazards with four radiation sensors: two dosimeters, a particle telescope, and a single event effect monitor. CEASE II contains an additional sensor, an electrostatic analyzer. These sensors are discussed in Section 3 of this report. CEASE's onboard data processing algorithms use these raw sensor outputs to provide real-time warnings to the spacecraft and operators, in physically meaningful engineering units.

### 2.1.1 Radiation Dose

As electronic components are exposed to ionizing radiation, they suffer progressive cumulative damage. Once a threshold dose for a given component is exceeded, its performance will degrade and the component may even fail catastrophically. The failure mechanism can depend on the total radiation dose, the radiation dose rate, or the type of particles responsible for the dose. For example, some components are particularly sensitive to displacement damage, a specific effect caused primarily by protons rather than electrons. The particle populations primarily responsible for radiation dose damage are  $>5$  MeV protons and  $>1$  MeV electrons. To better assess the radiation dose threats due to these particles, CEASE distinguishes proton and electron dose effects. The conditions at geosynchronous altitudes, in high inclination orbits following a major solar flare, and in the inner radiation belt present the most hazardous ionizing radiation doses for spacecraft.

CEASE measures *total radiation dose* (rads) and *dose rate* (rads/hr) with two independent dosimeters located behind planar aluminum (Al) shields. One shield is 0.08 inches (0.20 cm) thick and the other shield is 0.25 in (0.63 cm) thick. The smaller thickness represents a typical minimum shielding of spacecraft components (*Lightly Shielded Dose & Dose Rate*). The larger thickness is representative of well-shielded components (*Heavily Shielded Dose & Dose Rate*), since the dose-shielding depth curve changes slowly with shielding thickness above this value. CEASE measures separately the dose rates due to particles with Low and High Linear Energy Transfer (LOLET and HILET), to better characterize the radiation environment. These dosimeters are similar to many that have been flown since the 1960's.<sup>2</sup>

Radiation damage also dramatically compromises solar cell performance and lifetime. With its particle telescope, CEASE also measures the surface radiation dose that shortens the life of solar cells. Operators can use the *Surface Dose* register provided by CEASE to estimate the effect of the orbital environment on their solar cells. The surface dose data are obtained from both electrons and protons, and are quantified in units of equivalent fluence of 1 MeV electrons, a standard measure of dose damage to solar arrays.<sup>3</sup>

### 2.1.2 Single Event Effects

Very large energy deposition events create sufficient charge in an electronic device to alter its logic state, either temporarily (bit flip) or permanently (latch-up). The results are known as Single Event Effects (SEEs). SEEs can result in corrupted data processing, commanding, and telemetry. The worst cases can cause system failures. Typically, SEEs are induced by  $>50$  MeV proton or high energy heavy ions. The SEE hazard is greatest in the inner radiation belt. CEASE measures the rate of large energy deposition events ( $>25$  MeV) in a large volume diode ( $9 \times 9 \times 0.5$  mm<sup>3</sup>). Previous research has demonstrated that the SEE rate in a wide variety of devices is proportional to the rate of such large energy deposition events<sup>4</sup>.

### 2.1.3 Spacecraft Charging

Dielectric charging occurs when insulating materials absorb incident electrons. Surface charge can build on dielectric materials exposed to the space environment, leading to arc discharges. These discharges, in

---

<sup>2</sup> D.A. Hardy et. al., "The Space Radiation Dosimeter," in *CRESS/SPACERAD Experiment Descriptions* AFGL-TR-85-0017, p 175, and references therein.

<sup>3</sup> R.M. Sullivan, "Space Power Systems" in *Fundamentals of Space Systems*, V.L. Piscane and R.C. Moore, eds., Oxford University Press, 1994.

<sup>4</sup> Mullen, E.G., Ray, K.P., Koga, R., Holeman, E.G., and Delorey, D.E., "SEU Results from the Advanced Photovoltaic and Electronics Experiment (APEX) Satellite," *IEEE Transactions on Nuclear Science*, NS-42, 1988-1994, Dec, 1995.

Mullen, E.G., and Ray, K.P., "Microelectronics Effects as Seen on CRRES," *Advances in Space Research*, Vol.14, No. 10, 797-807, 1994.

turn, generate significant noise transients that upset or damage sensitive on-board electronics. Lower energy electrons drive the surface charging. Additionally, charge can build on dielectric materials (e.g. shielded electronics, coaxial cables) in the interior of a spacecraft. This phenomenon is known as deep dielectric charging and is caused by high energy electrons. Both types of dielectric charging are predominantly a hazard in high altitude and geosynchronous orbits, where the plasma density is relatively low. Both surface and deep dielectric charging are known to be a very real hazard to spacecraft and have led to numerous operational anomalies and even to the loss of spacecraft.<sup>5</sup>

CEASE monitors the environment causing both surface and deep dielectric charging with its particle telescope and, on CEASE II, the electrostatic analyzer. These sensors determine the energy spectrum of both electrons and protons, from which several parameters are deduced, including the probability of surface dielectric charging, and the probability of deep dielectric charging. CEASE monitors the environment causing spacecraft charging, the particles known to be responsible for charging, rather than directly measuring the surface potential on various materials. This measurement strategy is based upon extensive flight data, particularly that obtained on the USAF P78-2 SCATHA spacecraft. As is discussed in more detail in Section 4.3 of this report, flight data clearly show that:

- 1) Surface dielectric charging is due to a high flux of electrons with energy of tens of keV. This surface charging can cause discharges, which has been observed to cause transients and operational anomalies. *The presence of a high flux of electrons is sufficiently correlated with discharges to use this indicator as a basis for warnings for real-time satellite operations.*<sup>6</sup>
- 2) The flux of energetic electrons increases prior to charging, on a time scale ranging from minutes to an hour, while the charging is nearly simultaneous with the discharges and anomalies. *Monitoring the electrons therefore provides advance warning before potentially hazardous conditions occur, while monitoring the surface potential provides virtually no prior warning.*
- 3) Operational anomalies are at least as likely to be caused by deep dielectric charging as surface charging. The deep dielectric charging is caused by a high fluence of relativistic electrons, a flux that is elevated for days. Discharges due to deep dielectric charging are not associated with surface charging, thus a surface potential monitor does not warn of this hazardous condition.

The sensors and algorithms used by CEASE provide advance warning of spacecraft charging, from minutes to hours prior to hazardous conditions. This warning is based on the actual, measured, in-situ environment at the spacecraft and is not inferred from some global average of the environment or extrapolated from whatever spacecraft are nearby. CEASE provides a unique warning which gives operators the opportunity to alter spacecraft operations in ways that decrease the likelihood of a loss of service or other operational anomaly.

#### 2.1.4 On-board Processing

Efficient, modular software is one of the keys to the CEASE design. This allows the operator to have access to not just raw sensor data, but to valuable threat analysis as provided by CEASE onboard algorithms. Through the use of lookup tables to characterize the environment's threats, the onboard algorithms accommodate threat analysis for most orbital environments. Also, CEASE supports multiple spacecraft interfaces across which this information is supplied, providing even greater mission flexibility.

CEASE supports three telemetry streams: *Engineering*, *Science*, and *History*. The *Engineering* stream contains real-time warning and anomaly data, updated once per minute. *History* data contain finer resolution data, which can be used to support anomaly resolution. The *History* data are available for the preceding 72 hours in 15-minute blocks. *Science* Data packets contain proton and electron fluxes and energy spectra, radiation dose and dose rates. The *Science* Data update rate, or the *Science Data Interval*, is selected prior to instrument delivery from these options: 5, 10, 15, 20, 30 or 60 seconds. The *ESA* packet contains the *ESA* spectrum and *ESA* state-of-health information.

---

<sup>5</sup> Alan C. Tribble, *The Space Environment: Implications for Spacecraft Design*, Princeton University Press, 1995.

Daniel Hastings and Henry Garrett, *Spacecraft-Environment Interactions*, Cambridge University Press, 1996.

<sup>6</sup> H.C. Koons, D.J. Gorney, "Relationship Between Electrostatic Discharges on Spacecraft P78-2 and the Electron Environment", *Journ. Spacecraft and Rockets*, Vol 28, No. 6, p 683 (1991)

When CEASE is powered on, data are continuously collected from the sensors and processed by digital signal processing circuitry. After the *Science Data Interval* has elapsed, CEASE formats the raw data into a *Science Data* packet. CEASE performs further processing on the *Science Data* to produce two reduced data sets, *Engineering* and *History Data*. The *Engineering Data* are summed for 60 seconds, then formatted into the *Engineering Data* Packet. The *History Data* are summed for 15 minutes and then a *History Data* packet is created. The information in the *History Data* packets is not as detailed as in the *Science* packets and is not a substitute for *Science Data*.

All data types are continuously produced in CEASE and are always available. The spacecraft may acquire any or all of the data packets, as mission requirements dictate. The *Engineering Data* packet is updated once per 60 seconds by CEASE. If not retrieved by the spacecraft during this interval, the packet is overwritten with new data by CEASE at the end of the next interval. Similarly, the *Science Data* and *ESA* packets are updated and overwritten once per *Science Data Interval*. The History data are maintained in a 72-hour circular *History Buffer*. Every 15 minutes, CEASE transfers new History Data into the buffer, overwriting the oldest data in the buffer. To acquire *History Data*, a command is issued to CEASE which then transmits the selected data in its buffer to the spacecraft.

## 2.2 HAZARD REGISTERS AND WARNING FLAGS

The outputs of the onboard algorithms are the real-time warnings to the spacecraft of environmental hazards due to total radiation dose, radiation dose rate, surface and deep dielectric charging, and SEEs. This information is contained in eight 4-bit Hazard Registers (HR) and eight 1-bit Warning Flags (WF). The eight Hazard Registers each have 16 levels quantifying the environmental threat. These levels range from 0 to 15 (lowest to highest threat), with each Hazard Register having a lookup table. The Hazard Register levels (except for the SEE) are logarithmically spaced over a 5 decade dynamic range for LSD, HSD, LSR, HSR and SUD, and over a 4 decade range for SDC and DDC. The SEE Hazard Register is a direct count of SEE type events detected.

The specific values in the Hazard Register lookup tables are set prior to instrument fabrication to match mission requirements. In general, the Hazard Register and Fluence Flag limits will depend on the design of the spacecraft and its orbit. It is recommended that the spacecraft manufacturer discuss the mission profile with Amptek so that proper limits for Warning Flags can be determined.

The purpose of the Warning Flags (listed in Table 3) is to provide an ON/OFF hazard alert to the spacecraft. Six of the eight Warning Flags are derived from Hazard Register values. For these six flags, if a Hazard Register value exceeds a pre-set limit, the corresponding Warning Flag is set ON (1), and otherwise the Warning Flag is set OFF (0). The two additional flags are the *Electron Fluence Flags*, one for electrons with  $E < 250$  keV and one for  $E > 250$  keV. If the integrated electron SDC or DDC fluence over the past H hours exceeds the pre-set limit T, the corresponding fluence Warning Flag is set ON (1), otherwise it is set OFF (0).

Table 3. Warning Flag List

Warning Flag (Abbreviation)	Flag Number	Source Register	Trigger
Lightly Shielded Dose Rate (WLR)	0	HR <sub>3</sub>	HR <sub>3</sub> > Threat Level Threshold for 3 consecutive EMIs
Heavily Shielded Dose Rate (WHR)	1	HR <sub>4</sub>	HR <sub>4</sub> > Threat Level Threshold for 3 consecutive EMIs
Single Event Effect (WSE)	2	HR <sub>6</sub>	HR <sub>6</sub> > Threat Level Threshold for 3 consecutive EMIs
Surface Dielectric Charging Flux (WSC)	3	HR <sub>7</sub>	HR <sub>7</sub> > Threat Level Threshold for 3 consecutive EMIs
Surface Dielectric Charging Fluence (WSL)	4	—	If measured low energy electron fluence exceeds threshold for 3 consecutive EMIs
Deep Dielectric Charging Fluence (WDC)	5	HR <sub>8</sub>	HR <sub>8</sub> > Threat Level Threshold for 3 consecutive EMIs
Deep Dielectric Charging Flux (WDL)	6	—	If measured high energy electron fluence exceeds threshold for 3 consecutive EMIs
Total Dose (WTD)	7	HR <sub>1</sub> , HR <sub>2</sub> , HR <sub>5</sub>	HR <sub>1</sub> , HR <sub>2</sub> and/or HR <sub>5</sub> > their specific Threat Level Threshold for 3 consecutive EMIs

The on-board processing algorithm tracks the Warning Flag status. For a Warning Flag to be set, the corresponding Hazard Register or Fluence must exceed its preset limit for 3 minutes. For the *Electron Fluence Flags*, this means that the fluence values must exceed the preset limits for 3 consecutive minutes. For the WTD Flag, this requires that any combination of the applicable Hazard Registers (HR<sub>1</sub>, HR<sub>2</sub>, or HR<sub>5</sub>) exceeds the preset limits for 3 consecutive minutes.

The Warning Flag thresholds (0-15) can be set by ground command. A value of 15 is the default stored onboard CEASE for all Warning Flags except for the fluence flags. For the fluence flags, the fluence limit T and the value of H can be set by ground command. The value of H can be set between 1 and 24 hours in 1-hour increments. The default settings are H = 24 hours and the Fluence Flag limit =  $4 \times 10^9$ .

### 2.3 OPERATING CEASE

CEASE is designed to support several different operational strategies, depending on the mission requirements. It operates autonomously, without continuous telemetry transmission to the host spacecraft. CEASE always processes the raw data it collects from its sensors and prepares all of the data packets at the specified rates. CEASE only transmits the prepared packets upon request from spacecraft.

In highly autonomous operation, the spacecraft reads the ten byte Engineering data and the single byte of Warning Flags is evaluated by the spacecraft's onboard processor. If all bits are zero, no further action need be taken. If a bit is nonzero, indicating a hazardous condition, then the complete ten byte Engineering Data Packet can be transmitted to the ground. Spacecraft operators can take appropriate action, including acquiring Science or History data from CEASE. Further autonomy can be achieved if the spacecraft processor uses the threat analysis real-time to inhibit critical commands until the threat diminishes.

If sufficient telemetry bandwidth is available, complete Engineering and Science Data can be continuously read by the spacecraft and transmitted to the ground. This provides the most complete data set. But where telemetry bandwidth is limited, satellite controllers have the option of only requesting data from CEASE when there is interest. In this alternative, only the ten byte Engineering data are read by the spacecraft and transmitted to the ground, to provide a summary of the environment. If Engineering data alert

the operators to a hazardous condition, the operators can then choose to acquire the Science Data and transmit it to the ground. For anomaly resolution, controllers could request History Data only, for the relevant time interval. Or during severe geomagnetic storm conditions, controllers could request Science Data to obtain the most information possible.

### 3 SENSOR RESPONSE: MODELS, TESTS, AND CALIBRATION

As part of the support effort described here, the response of the CEASE sensors to energetic particles was modeled and calibration data obtained. Understanding this response is critical to interpreting the CEASE data and to implementing the onboard data processing algorithms.

#### 3.1 DOSIMETERS

CEASE has two dosimeters, termed DD1 and DD2. Both are Si-PIN photodiodes, located under planar shields, which is typical of the radiation shielding provided for spacecraft electronics. DD1 is located below 0.080" Al while DD2 is located below 0.250" Al. By definition, radiation dose is deposited energy per unit volume. Therefore, by measuring the deposited energy we obtain directly the dose. In addition to determining the total dose, the dosimeters provide some information on the identity and energy spectrum of the particles responsible for the dose. CEASE measures separately the counts and dose for particles with Low Linear Energy Transfer (LOLET) and High Linear Energy Transfer (HILET), subdividing the HILET range into HILET-A and HILET-B.

The boundaries between the LOLET and HILET ranges are shown in Table 4. The values for CEASE S/N 002 differ from those of S/N 001, which is considered to be the standard and will be used in future instruments. The geometric factor of the dosimeters is the product of the area (0.81 cm<sup>2</sup>) and the angle (2π ster), 5.1 cm<sup>2</sup>-ster.

Table 4. Table of LOLET/HILET Boundaries

DD1		DD2		Deposition Threshold	
Incident Energy (MeV)		Incident Energy (MeV)		Deposited Energy (MeV)	
Min	Max	Min	Max	Min	Max

S/N 002

LOLET Electrons	1.0		2.5		0.050	0.085
LOLET Protons	78.0		86.0		0.050	0.085
HILET A Protons	26.5	78.0	41.7	86.0	0.085	3.0
HILET B Protons	19.6	26.5	37.2	41.7	3.0	10.0

Standard (S/N 001)

LOLET Electrons	1.0		2.5		0.050	1.0
LOLET Protons	64.0		73.0		0.050	1.0
HILET A Protons	26.5	64.0	41.7	73.0	1.0	3.0
HILET B Protons	19.6	26.5	37.2	41.7	3.0	10.0

The deposited energy thresholds are measured. The incident energy values are computed, for orthogonally incident particles, using a continuous slowing down approximation. For protons, this approximation is quite accurate. The proton calculation is based up the Janni tables. For electrons, this approximation only provides a "mean" result, since scattering is a major effect ignored in the present calculation. The electron results differ in two important ways from a simple calculation. First, electrons with low energy are stopped in the Al shielding. For example, an electron with energy <1 MeV cannot pass through 80 mils of Al so cannot reach DD1. However, in the process of stopping, such an electron will emit

brehmstrahlung X-rays, which can pass through the Al and reach DD1. The lower energy threshold for the electron is therefore, in practice, lower than that shown in Table 4. Second, a high energy electron can scatter several times in passing through a dosimeter diode. There is a small but nonzero probability that it will have a long and "tortured" path through the diode, thereby depositing much more energy than is computed from a naïve, continuous slowing down approximation and thereby registering in the HILET channels.

The CEASE dosimeter calibrations carried out under this contract focused on verifying the dose measurements. Small, calibrated  $\gamma$ -ray sources were used to verify that the total dose measured by the CEASE system (sensor, electronics, and data processing algorithm) matched the total dose measured by more conventional sensors and known from the calibration.

### 3.2 TELESCOPE

#### *Sensor Description*

The energetic particle telescope consists of two coaxial solid state detectors, a front detector (DFT) and a back detector (DBT). Penetrating particles (electrons and protons) deposit energy in DFT only or in both DFT and DBT. The pattern of energy deposited in the two detectors depends on the particle species and energy. The data processing algorithms for the telescope perform particle identification and energy measurement by using the pattern of energy deposition in the telescope detectors. There are 80 possible digitized pulse height values for any particle incident on the telescope detectors: 8 possible values if the particle strikes DFT only, 8 if DBT only and 64 if there is a coincident hit on both DFT and DBT. Thus all incident particle counts can be stored in these 80 bins, called Logic Boxes (LB).

DFT has 25 mm<sup>2</sup> nominal active area and is 150  $\mu$ m thick, while DBT has 50 mm<sup>2</sup> nominal area and is 700  $\mu$ m thick. The true electrically active area was found to be larger than the "nominal" are specified by the manufacturer, with an electrically active radius that is approximately 1.2 mm larger than the radius determined from the nominal area. It is worth noting that future telescopes will utilize a 500  $\mu$ m thick DBT, because the 700  $\mu$ m thick detector has limited availability.

The detectors are located inside a copper enclosure which absorbs protons with  $E < 60$  MeV and electrons with  $E < 8$  MeV. A front tungsten disk, coaxial with the detectors, has a small aperture (0.023 cm radius). In front of this is a copper collimator with an field-of-view opening half angle of 45°. A 9  $\mu$ m thick Al foil covers the aperture to make it light tight. It is these collimators, rather than the detector areas, which define the opening angle for protons that do not penetrate the tungsten. The foil and the electronic circuit threshold determine the low energy cut-offs for the telescope: 45 keV for electrons and 700 keV for protons.

Table 5. Telescope geometric quantities primarily responsible for sensor response

	Area (cm <sup>2</sup> )	Radius	Depth (from foil)	Thickness	Thickness (g/cm <sup>2</sup> )
Al Foil				0.0009 cm	2.4x10 <sup>-3</sup>
W collimator	1.66x10 <sup>-3</sup>	0.009" 0.023 cm		0.020" 0.050 cm	9.6x10 <sup>-1</sup>
DFT - Si	Nominal: 25 Actual: 50	0.282+ 0.12 cm	0.075" 0.191 cm	150 $\mu$ m	3.5x10 <sup>-2</sup>
DBT - Si	Nominal: 50 Actual: 85	0.399+ 0.12 cm	0.234" 0.594 cm	700 $\mu$ m (500 $\mu$ m)	1.6x10 <sup>-1</sup>

#### *Computed Response*

Figure 1 is a plot of the expected response of the CEASE particle telescope to protons and electrons. This plot shows the energy deposited in the front and rear detectors as a function of particle, for protons and electrons, as a function of energy. The proton curve is the larger one, on the upper right, with arrows at 5, 11, 20 MeV, etc. The electron curve has its peak at 600 keV. As discussed in the dosimeter response

section, electron scattering is important. The small numbers in each LB indicate the lowest energy electrons produce a significant fraction of counts in that LB.

The two species have significantly distinct energy deposition patterns, permitting CEASE to reliably distinguish the two. The different energies are also distinct, permitting CEASE to measure the energy spectra. Along with the deposition patterns are shown the energy boundaries of the LBs used to characterize the telescope data.

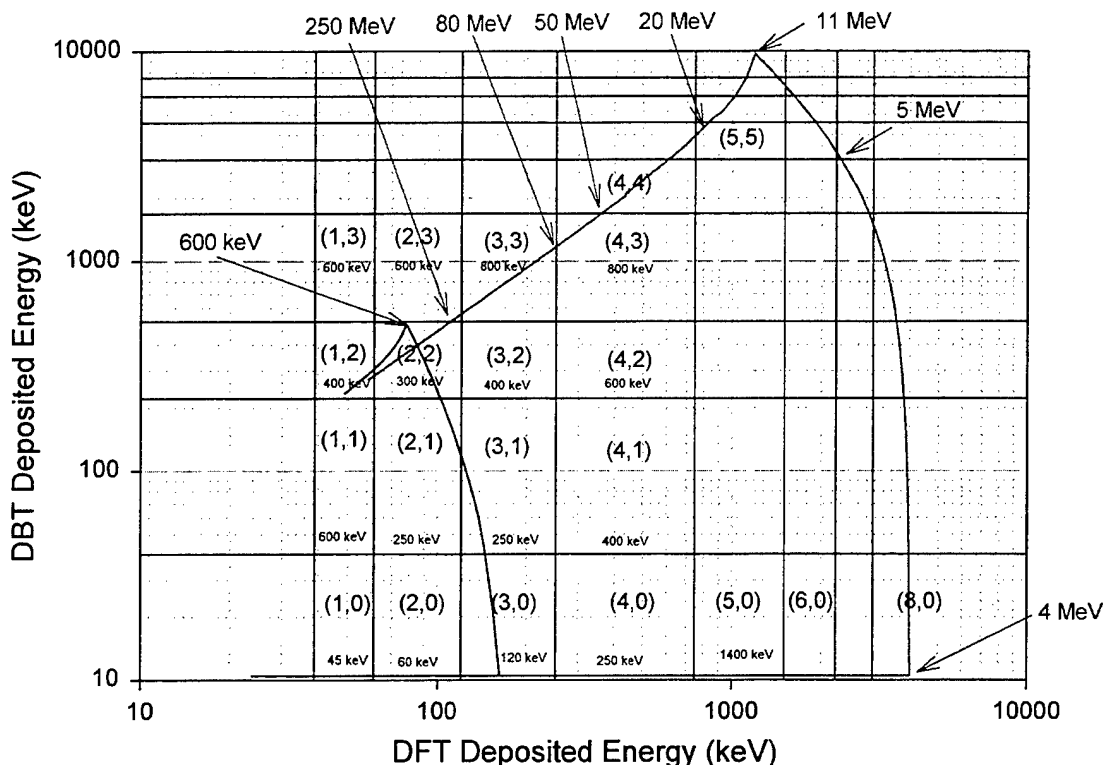


Figure 1. Plot showing the computed pattern of energy deposition in the CEASE particle telescope.

Both the proton and electron curves shown represent the most probable values for the depositions. The actual energy deposited by the protons is very close to that shown here. Some fluctuation about the curve is observed, but it is minimal. For electrons, however, the actual pattern of deposition at a particular energy is very broad, because electrons are light particles that scatter broadly. The general distribution is as shown here, but at any single energy, a significant fraction of the electrons will fall into adjacent boxes. For this reason, various logic box counts are combined to give an estimate of the particles within fairly broad ranges. For electrons, CEASE returns the flux of electrons with  $50 \text{ keV} < E < 250 \text{ keV}$  (LBs (1,0), (2,0), and (3,0)) and of high energy electrons with  $E > 250 \text{ keV}$ . However, CEASE cannot easily distinguish the lower and higher energy protons of the high-energy electron range.

The CEASE telescope will respond to penetrating, very high energy, out of aperture protons. The tungsten disk has a thickness of 20 mils = 0.05 cm, corresponding to a proton range of 19.4 MeV. Protons with an energy  $> 20 \text{ MeV}$  will pass through the tungsten and reach the detectors. The geometric factor for penetrating particles is determined by the geometry of the detectors, with a solid angle exceeding that defined by the collimator. CEASE therefore has an enhanced response to very energetic protons. The CEASE telescope also responds to very energetic electrons. All straight line trajectories that pass through the collimator opening and DBT also pass through DFT. However, some energetic electrons may trigger only DBT, by wide angle scattering and by the production of brehmstrahlung in the shield and collimator. Because of the much larger volume of DBT, brehmstrahlung X-rays have a much large probability of interacting in DBT, creating a high DBT single rate.

## Calibrations

Calibrating the as-built telescopes and testing the onboard data processing algorithms was an important component of the support effort. Figure 2 shows the effective area and the angular response measured with the flight telescopes. The angular response for both protons and electrons is somewhat greater than that computed from the simple geometry, due to scattering. The energy dependent, effective geometric factor (GF) of the telescope is computed by folding the effective sensitive area of the telescope with the angular response. The limiting GF values for the two calibrated CEASE units are  $1.6 \times 10^{-3} \text{ cm}^2\text{-sr}$  for electrons and  $7.6 \times 10^{-4} \text{ cm}^2\text{-sr}$  for protons (0.045 cm diameter collimator aperture).

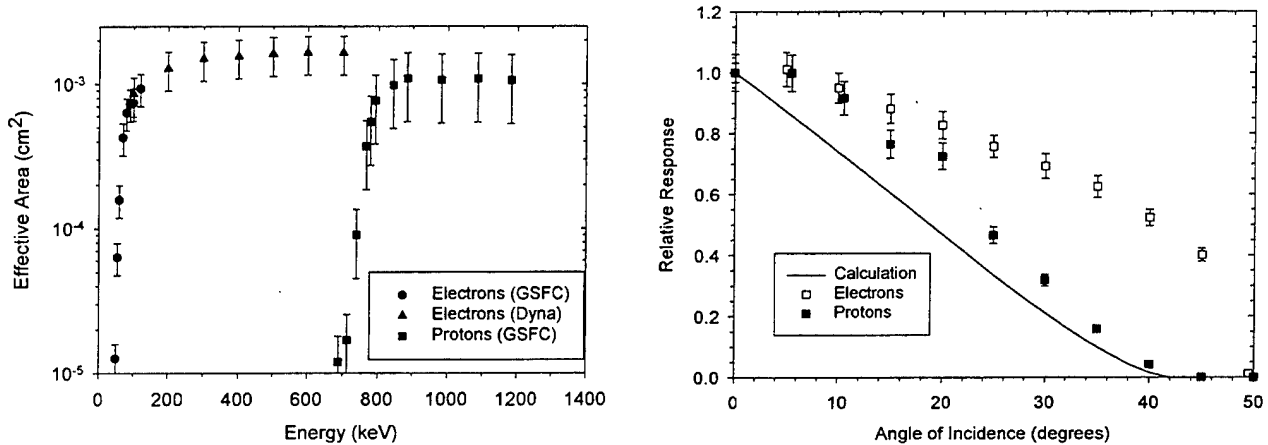


Figure 2. CEASE Telescope Effective Area and Angular Response

The patterns of electron and proton energy deposition were measured in beam calibrations. The proton data agree very well with the Janni model, as expected, so are not shown here. Plots of the pattern of energy deposition from electrons at four different energies are shown in Figure 3. These data were all obtained at the Van de Graaf accelerator at Goddard Space Flight Center. At 175 MeV, which is below the energy at which electrons will punch through DFT, 85% of the counts wind up in the LB where one would expect. Some counts are observed in both DFT and DBT. This is due to brehmstrahlung X-rays, produced when electrons stop in DFT, which reach DBT.

At 300 MeV, which is high enough for electrons to punch through DFT, the scattering is very noticeable. 60% of the electrons are still stopped in DFT. At 800 MeV, 25% of the electrons are still stopped in DFT. A naïve algorithm counts these as electrons less than 250 keV. Some counts are recorded in essentially all boxes where the DFT+DBT total is less than 800 keV. A significant number of interactions are observed in DBT only. These presumably result from electrons that scatter in the collimator and the material around DFT such that they reach DBT without passing through DFT. The pattern at 1,200 keV is not very different from that observed at 800 keV: there is a slightly higher fraction of the counts near the end of the electron curve.

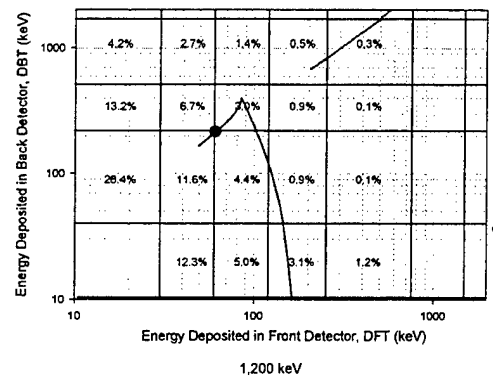
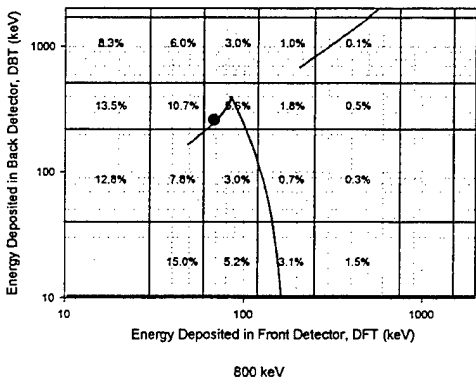
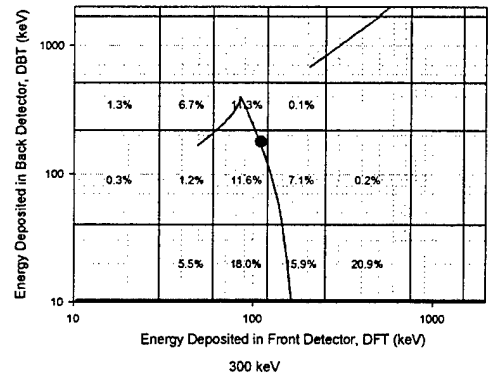
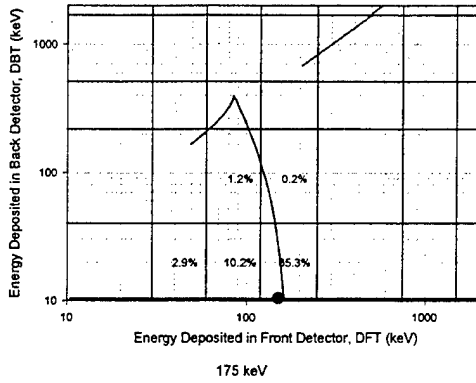


Figure 3. Measured patterns of electron energy deposition in CEASE Telescope. The black dot indicates the energy deposition calculated from range-energy considerations, neglecting scattering.

### 3.3 SEE SENSOR

The SEE detector consists of a photodiode identical to that used for DD1 and DD2. The primary difference is that the SEE detector is connected to a discriminator with a large energy deposition threshold, approximately 25 MeV. The SEE sensor counts the number of times an energy of 25 MeV is deposited in this volume. This corresponds to a LET of 215 MeV/g-cm<sup>2</sup>. Such a large energy deposition will usually occur only when a nuclear interaction occurs in the photodiode, although massive cosmic rays can deposit such large energies. The output of the SEE sensor is the total number of such large energy deposition events, the counts, in the Engineering Mode Interval (EMI), typically 60 seconds. In CEASE S/N 002, the counter has a maximum value of 15. In CEASE S/N 001 and in all later units, the counter has an optional prescaler permitting up to 256 counts in an EMI.

Figure 4 shows a simple model of the probability of a nuclear scattering event in silicon, for protons, as a function of incident proton energy. The cross-section is vanishing for an energy incident on the diode below 20 MeV. To reach the SEE detector with 20 MeV incident energy, a proton must have an energy of 40 MeV incident on CEASE. Thus the SEE detector responds to protons above 40 MeV, with a response that increases up to an asymptotic limit around 200 MeV and above. The probability of upset in electronic devices increases similarly. For calibration, the analog electronics include a switch to reduce the threshold to 1 MeV, with a corresponding LET of 9 MeV/g-cm<sup>2</sup>. A <sup>60</sup>Co source is used to verify the 1 MeV threshold.

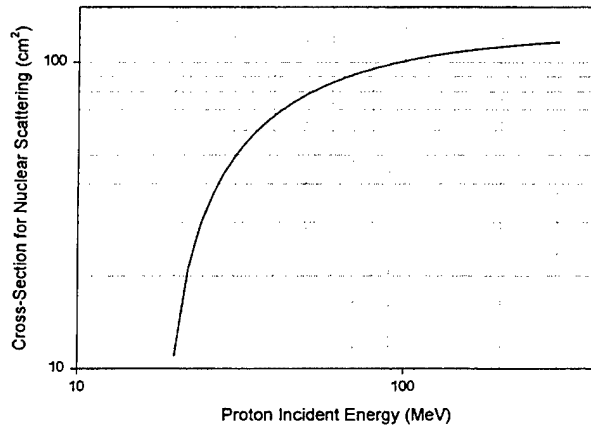


Figure 4. Computed probability of a nuclear scattering event in Si, as a function of energy.

## 4 FLIGHT SOFTWARE

### 4.1 STATUS REGISTER ALGORITHMS

The following is a summary of the algorithms used in computing Status Register values. The thresholds given in this section are nominal values, which were used in both S/N 001 and 002 as supported by this contract. They can be customized for specific future missions.

#### *Radiation Dose Calculation*

The radiation dose in rads is defined as 100 ergs of absorbed radiation per gram of absorbing substance, or 1 rad = 100 erg/g =  $6.24 \times 10^7$  MeV/g. Equivalently, we can write

$$\text{Dose (rads)} = 1.602 \times 10^{-8} \frac{\Delta E (\text{MeV})}{m (\text{g})}$$

where  $\Delta E$  is the energy deposited in the detector in MeV and  $m$  is the detector mass. Similarly, we can write an equation for the dose rate (rads/hr)

$$\text{DoseRate (rads/hr)} = 5.77 \times 10^{-5} \frac{\delta E (\text{MeV/sec})}{m (\text{g})}$$

where  $\delta E$  is the energy deposited per second in the detector. The sensitive mass for a detector is given by  $m = \rho \cdot A \cdot t$  where  $\rho$  is the density ( $2.33 \text{ g/cm}^3$  for Si),  $A$  is the active area of the detector and  $t$  is the depletion depth. The sensitive mass varies for each detector type. For the CEASE dosimeters, detectors  $A = 0.81 \text{ cm}^2$  and  $t = 500 \text{ } \mu\text{m}$ , thus giving  $m = 0.094 \text{ g}$ . For a proton depositing 1 MeV, the incremental dose is  $1.7 \times 10^{-7}$  rads.

#### *Lightly Shielded Dose Status Register (LSD - SR1)*

SR1 yields the total radiation dose received by electronic devices shielded behind an equivalent of 0.08" of aluminum. This register is useful in determining when lightly shielded electronic components are reaching the limits of their radiation hardness.

There are four outputs from DD1, the lightly shielded dosimeter: the number of LOLET counts (LLC), the number of HILET counts (HLC), the LOLET dose (LLD), and the HILET dose (HLD). These four values are summed over an Engineering Mode Interval (EMI), nominally 60 seconds. The incremental dose delivered in that EMI is then computed as

$$\Delta C_1 = 2C_t(\text{LLD} + 10 \cdot \text{HLD})$$

where the factor of 2 is a 50% duty cycle correction, the factor of 10 accounts for the difference in HILET and LOLET gain, and  $C_t$  is a dead time correction factor, determined from  $\text{LLC} + \text{HLC}$ , the total count rate in DD1. The total dose in DD1 is found by adding  $\Delta C_1$  to the previous value for  $C_1$ . The value in  $\text{SR}_1$  is given by

$$\text{SR}_1 = 5 \log_{10}(C_1 / B_1)$$

where  $C_1$  is the total dose measured in DD1, integrated since instrument turn-on;  $B_1$  is the threshold dose, nominally 187 rads; and the factor 5 determines the dynamic range of measurement.

Since the instrument may be turned off and then back on in orbit, CEASE includes a command to set a DD1 total dose value. The incremental dose in each subsequent EMI will be added to this.

#### *Heavily Shielded Dose Status Register (HSD - SR2)*

The total radiation dose received by electronic devices shielded behind an equivalent of 0.25" of aluminum. This register is useful in determining when relatively heavily shielded electronic components are reaching the limits of their radiation hardness. The processing for HSD is entirely analogous to that of LSD, except that the data come from DD2 instead of DD1, and the threshold dose is 93 rads, since lower doses are expected behind the additional shielding.

### *Lightly Shielded Dose Rate Status Register (LSR - SR3)*

The total radiation dose rate received by electronic devices shielded behind an equivalent of 0.08" of aluminum during the last EMI. This register is useful in determining when dose rate effects may affect lightly shielded electronic components. The dose rate in DD1 in the last EMI is  $\Delta C_1/\Delta T$ , the incremental dose in DD1 divided by the duration of an EMI. The value in  $SR_3$  is given by

$$SR_3 = 5 \log_{10}(C_3 / B_3)$$

where  $C_3 = \Delta C_1$ , the incremental dose in DD1;  $B_3$  is the threshold dose rate, 43 millirad/hr; and the factor 5 determines the dynamic range of measurement.

### *Heavily Shielded Dose Status Register (HSR - SR4)*

The total radiation dose received by electronic devices shielded behind an equivalent of 0.25" of aluminum during the last EMI. This register is useful in determining when dose rate effects may affect heavily shielded electronic components. The processing for HSD is identical to that of LSD.

### *Solar Cell Damage Status Register (SUD - SR5)*

The total radiation dose received by devices with a minimum amount of shielding, such as solar panels. This register is useful in determining the expected efficiency of solar panels through the duration of a mission. The effect of ionizing radiation on solar cells is quantified, in engineering terms, in units of the "equivalent unidirectional fluence of 1 MeV electrons" (EF)<sup>7</sup>. Omni-directional particle flux, for any particle species at any energy, can be converted to EF using an empirically determined, damage factor,  $DF(E,p)$ . The value of DF depends both on the particle type, p, and its energy, E. Typically, no significant degradation of solar cell power output is seen for EF fluences below  $10^{14}$  electrons/cm<sup>2</sup> and significant degradation (> 50%) is seen for EF fluences greater than  $10^{16}$  electrons/cm<sup>2</sup>. Damage factors depend on the cover glass thickness, since the glass shields the solar cell material from the lowest energy electrons and protons. The nominal CEASE algorithm assumes a 6 mil (0.015 cm) thick cover glass and silicon solar cells.

The CEASE telescope measures the energy spectrum of incident protons and electrons by measuring the energy deposited in the front and back detectors and binning the deposited energy into 80 Logic Boxes (LBs). These counts in the 80 LBs are summed over an Engineering Mode Interval (EMI), nominally 60 seconds. To determine the EF, the counts in LBs corresponding to protons with  $E > 4$  MeV and electrons with  $E > 250$  keV are used. The counts in each LB are multiplied by appropriate geometric factors and damage factors, then summed into an incremental fluence,  $\Delta EF$ . This is then multiplied by  $C_t$ , a dead time correction factor, determined from the sum of the counts in all 80 LBs.

$$\Delta EF = C_t [\sum LB(i,j) DF(i,j)]$$

where the sum is taken over the proper logic boxes. The total equivalent unidirectional fluence of 1 MeV electrons is found by adding  $\Delta EF$  to the previous value for EF. The value in  $SR_5$  is given by

$$SR_5 = 4 \log_{10}(C_5 / B_5)$$

where  $C_5$  is the total equivalent unidirectional fluence of 1 MeV electrons, integrated since instrument turn-on;  $B_5$  is the threshold fluence,  $1.76 \times 10^{13}$  electrons/cm<sup>2</sup>; and the factor 4 determines the dynamic range of measurement.

### *Single Event Effect Status Register (SEE - SR6)*

The value of this register corresponds to the expected number of upsets/bit/day of a typical IC as a result of bombardment by high-energy protons and heavy ions. This flag is useful in identifying the times when the SEE probability is high. Critical activities, such as attitude control commanding, should be avoided at such times. This register is a straight count of SEE-like events from DD3 within the Engineering Mode Interval of 1 minute. A value of 15 is reported if the counts are greater than or equal to 15 within 1 minute. If the DD3 threshold is Normal, this is then a count of all events above the threshold of 50 MeV. If the DD3 threshold is Low, this is a count of all events above the 1 MeV threshold. As an option, scaling of the SEE-

<sup>7</sup> R.M. Sullivan, "Space Power Systems" in *Fundamentals of Space Systems*, V.L. Piscane and R.C. Moore, eds., Oxford University Press, 1994.

like events is available. If it is used, then the LS 3 bits of the SR<sub>6</sub> scale factor are downlinked in Status Byte 1 and SR<sub>6</sub> equals the 8 bit SEE counter divided by 2<sup>3</sup>(scale factor).

*Surface Dielectric Charging Status Register (SDC - SR7)*

The value of this register is proportional to the threat level of charging of dielectric materials near the spacecraft surface (thermal blankets, exposed wires). This flag is useful in identifying the times when electric discharges at the SC surface may occur. These discharges may damage delicate surfaces and introduce noise and spurious signals into the SC circuitry. This register's value is determined from particle telescope data. The counts in each LB corresponding to electrons with 50 keV < E < 250 keV are summed over an EMI, multiplied by appropriate geometric factors, multiplied by a dead time correction factor, and then summed over the logic boxes,

$$C_7 = C_i [\sum LB(i,j) DF(i,j)]$$

where the sum is taken over the proper logic boxes. The value in SR<sub>7</sub> is given by the formula

$$SR_7 = N \log_{10}(C_7 / B_7)$$

where B<sub>7</sub> is the threshold flux; electrons/cm<sup>2</sup>; and the factor N determines the dynamic range of measurement, where B<sub>7</sub> = 5.0x10<sup>4</sup> electrons/cm<sup>2</sup>-sec and N=3.

*Deep Dielectric Charging Status Register (DDC - SR8)*

The value of this register corresponds to the threat level of charging of dielectric materials in the interior of the spacecraft. This flag is useful in identifying the times when electric discharges in well-shielded electric signal cables may occur. These discharges may introduce noise and spurious signals into the SC circuitry. The processing for DDC is entirely analogous to that of SDC, except that the data come from the LBs corresponding to electrons with E>250 keV, and the threshold flux is B<sub>8</sub> = 4.2x10<sup>3</sup> electrons/cm<sup>2</sup>-sec.

*Dead Time Corrections*

This section describes the effects of measured CEASE dead times on the storage and processing of CEASE Science, Engineering and History Data. The telescope dead time can be described with a non-paralyzable model with a 3 μsec dead time, τ<sub>Tel</sub> = 3 x 10<sup>-6</sup> sec. The dosimeter dead time can be described with a non-paralyzable model with a 7 μsec dead time, τ<sub>Dos</sub> = 7 x 10<sup>-6</sup> sec. The non-paralyzable dead time model is described by the following equations:

$$N = CF * M \qquad CF(M, \tau) = \frac{1}{1 - M \cdot \tau}$$

where N is the true input count rate, M is the measured count rate, and τ is the dead time. The measured count rate is a function of the true input count rate and the system dead time resulting from the limits of the pulse processing electronics. The dead time correction factors used for Engineering and History data are as follows:

Table 6. Dead time correction factors used in CEASE algorithms

Detector	Measured Count Rate (M)	Correction Factor
Telescope	M < 67 kHz	1.0
	M > 67 kHz	1.5
Dosimeters	M < 29 kHz	1.0
	29 < M < 61 kHz	1.5
	61 < M < 79 kHz	2.0
	M > 79 kHz	3.0

#### 4.2 CONVERSION TO ENGINEERING UNITS

The following table provides the conversion between Engineering Data values and the corresponding physical quantities, in engineering units, for the CEASE delivered units. These values can easily be altered for future missions. In each case, this table provides the lower limit corresponding to a given status register value. That is, if SR<sub>1</sub> reads 2, then the dose to lightly shielded components is between 296 and 469 rads. The Warning Flags have the same conversion: if the threshold for Warning Flag 0 is set to 2, and if the dose exceeds 296 rads for 3 consecutive engineering mode intervals (60 sec each), Warning Flag 0 is set ON (1)

Note that SR3 and SR4 have the same conversion factors. Two columns are shown, giving units of both rads/hr and rads/yr. The conversions listed here are for the standard look-up tables.

Table 7. Conversion between Engineering Data values and Physical Quantities in Engineering Units

Status Register	1	2	3 & 4	3 & 4	5	6	7	8
	Light Shield Dose	Heavy Shield Dose	Dose Rates	Dose Rates	Solar Cell Damage Factor		Surface Dielectric Charging	Deep Dielectric Charging
Acronym	LSD	HSD	LSR & HSR	LSR & HSR	SUD	SEE	SDC	DDC
Units	rad	rad	rad/hr	rad/yr	elec/cm <sup>2</sup>	min <sup>-1</sup>	elec/cm <sup>2</sup> -sec	elec/cm <sup>2</sup> -sec
0								
1	187	93	0.04	377	1.8 x 10 <sup>13</sup>	1	5.0 x 10 <sup>4</sup>	4.2 x 10 <sup>3</sup>
2	296	148	0.07	597	3.1 x 10 <sup>13</sup>	2	1.1 x 10 <sup>5</sup>	9.0 x 10 <sup>3</sup>
3	469	235	0.11	946	5.6 x 10 <sup>13</sup>	3	2.3 x 10 <sup>5</sup>	1.9 x 10 <sup>4</sup>
4	744	372	0.17	1,500	9.9 x 10 <sup>13</sup>	4	5.0 x 10 <sup>5</sup>	4.2 x 10 <sup>4</sup>
5	1,179	589	0.27	2,377	1.8 x 10 <sup>14</sup>	5	1.1 x 10 <sup>6</sup>	9.0 x 10 <sup>4</sup>
6	1,869	934	0.43	5,970	3.1 x 10 <sup>14</sup>	6	2.3 x 10 <sup>6</sup>	1.9 x 10 <sup>5</sup>
7	2,962	1,480	0.68	9,462	5.6 x 10 <sup>14</sup>	7	5.0 x 10 <sup>6</sup>	4.2 x 10 <sup>5</sup>
8	4,695	2,346	1.08	14,966	9.9 x 10 <sup>14</sup>	8	1.1 x 10 <sup>7</sup>	9.0 x 10 <sup>5</sup>
9	7,441	3,718	1.71	23,767	1.8 x 10 <sup>15</sup>	9	2.3 x 10 <sup>7</sup>	1.9 x 10 <sup>6</sup>
10	11,793	5,893	2.71	37,688	3.1 x 10 <sup>15</sup>	10	5.0 x 10 <sup>7</sup>	4.2 x 10 <sup>6</sup>
11	18,690	9,340	4.30	59,700	5.6 x 10 <sup>15</sup>	11	1.1 x 10 <sup>8</sup>	9.0 x 10 <sup>6</sup>
12	29,622	14,803	6.82	94,618	9.9 x 10 <sup>15</sup>	12	2.3 x 10 <sup>8</sup>	1.9 x 10 <sup>7</sup>
13	46,947	23,461	10.80	94,618	1.8 x 10 <sup>16</sup>	13	5.0 x 10 <sup>8</sup>	4.2 x 10 <sup>7</sup>
14	74,406	37,183	17.12	149,959	3.1 x 10 <sup>16</sup>	14	1.1 x 10 <sup>9</sup>	9.0 x 10 <sup>7</sup>
15	117,926	58,931	27.13	237,669	5.6 x 10 <sup>16</sup>	15	2.3 x 10 <sup>9</sup>	1.9 x 10 <sup>8</sup>

#### 4.3 RATIONALE FOR CHARGING ALGORITHMS

The algorithms used for the dosimetry, including surface dosimetry, and for single event effects, are based on methods and flight data that relatively well accepted. References for these algorithms have already been given in this report, in Sections 2.1.1, 2.1.2, and 4.1. However, there exists significant debate in the technical literature on the best methods to evaluate charging hazards. It therefore seems worthwhile

to review the rationale behind CEASE's charging algorithms. Note that the purpose of CEASE is to provide operational advance warnings, not to support research on the degree of charging.

The most definitive research on spacecraft charging and associated anomalies is based upon data obtained using the P78-2 (SCATHA) spacecraft. There are three main points from the SCATHA charging data, which were stated previously and are the basis for the CEASE design. We repeat them here, then present the technical references that support these points.

1) Surface dielectric charging is due to a high flux of electrons with energies of tens of keV. This surface charging can cause discharges, which can cause transients and operational anomalies. The presence of a high flux of electrons is sufficiently correlated with discharges to use this indicator as a basis for warnings for real-time satellite operations.

2) The flux of energetic electrons increases prior to charging, on a time scale ranging from minutes to an hour, while the charging is nearly simultaneous with the discharges and anomalies. Monitoring the electrons therefore provides advance warning before potentially hazardous conditions occur, while monitoring the surface potential provides virtually no prior warning.

3) Operational anomalies are at least as likely to be caused by deep dielectric charging as surface charging. The deep dielectric charging is caused by a high fluence of relativistic electrons, a flux that is elevated for days. Discharges due to deep dielectric charging are not associated with surface charging, thus a surface potential monitor does not warn of this hazardous condition.

#### **4.3.1 Surface Charging**

##### *Correlation of Surface Charging with Electron Flux*

- Adamo [1983] showed quite clearly that many transient pulses were associated with surface charging.
  - o Specifically, the data in the transient pulse monitor often correlated with surface potential monitor measurements of differential and absolute charging.
  - o Different materials and locations on the spacecraft charged differently. Sometimes discharges were associated with Kapton charging, sometimes with Teflon charging, sometimes with other materials.
  - o Charging properties changed over time. Early in the mission, Kapton charged up more readily than Teflon. Later in the mission, under exactly the same environmental conditions, Teflon charged to a higher potential.
- Koons [1983] showed that the transient pulses were often associated with surface charging, and further showed that the surface charging associated with transient pulses were preceded by increases in the flux and mean energy of electrons in the tens of keV.
- Koons [1988] also showed that surface charging was preceded by an increase in the flux of energetic electrons. The best predictor he found was the flux of 140 keV electrons.
- Mizera [1983] showed that the electron current, integrated from 5 to 80 keV, is the dominant contributor to surface charging and "is a sensitive indicator of the magnitude of the charging". This data focused on charging in shadow, either in eclipse or during spacecraft spin.
- Mullen [1986] concentrated on charging in daylight, and showed similarly that the electron current, integrated above 30 keV, was well correlated with charging.

##### *Energy Range of Electrons Associated with Surface Charging*

- The fact that the energetic electrons, in the tens of keV range, cause charging is somewhat of a surprise. It is generally agreed that most of the electron current is carried at lower energies, but that the magnitude of the charging depends on the high energy tail of the electron distribution. This is the conclusion of Mizera [1983], Koons [1988], and Mullen [1986].
- Mullen [1986] provides a possible explanation: the lower energy electrons cause secondary emission and so the currents into and out of the surface are self-balancing. Electrons in the tens of keV range deposit energy deep enough in the surface materials that there is little secondary emission and hence cause charging.

### *Prediction of Surface Charging*

- Several authors looked at the best predictors for surface charging. There was some correlation with magnetospheric activity (i.e.  $K_p$ ) and with local time and so on. But the best indicator was the electron flux.
- According to Koons [1991], the incidence of internal discharges at daily electron fluences above  $10^{10}$  per  $\text{cm}^2$  is sufficiently high to warrant the use of this indicator to issue warnings for real-time satellite operations.
- Based on the difficulty of directly measuring the charging at a large number of locations on a spacecraft surface, with a large number of materials, we at Amptek concluded that measuring the energetic electron flux provided the best method for warning of possible charging conditions.

#### **4.3.2 Electron Flux Provides Advance Warning**

A primary advantage of using the measured electron flux rather than a surface potential monitor to assess charging hazard is that the electron flux enhancement precedes the discharge, while the charging occurs nearly simultaneously with the discharge. There are several papers where this is clear from an examination of the figures, though not explicitly stated in the text.

- Koons [1988] showed clearly that the discharges were nearly simultaneous with the peaks in surface potential, to within a minute. In fact, several discharges occurred during the time that the surface potential was increasing. These discharges followed an hour of sustained energetic electron flux.
- Mullen [1986] showed that the flux prior to charging increased by a factor of 10 to 20 over the normal baseline flux, for anywhere from 15 to 60 minutes prior to the charging events.
- Garret [1981] showed that the dielectric surfaces on the spacecraft charge up with a time scale that can range from tens of minutes to days. That is, when there is a sustained enhancement in the electron flux, surface charging follows it by tens of minutes or longer
- Both Mizera [1983] and Koons [1983] showed that the surface charging followed the electron flux enhancement by anywhere from a few minutes to an hour.

Spacecraft operators can take action to minimize the possibility of loss of service, by placing additional assets on a standby basis. They can also minimize the possibility of damage to the spacecraft, by limiting commands that could be distorted by transient pulses. However, to take these actions they need advance warning. We at Amptek feel that the data show very clearly that the flux of energetic electrons provides advance warning, with a time scale sufficient to take actions, while the surface potential occurs simultaneously with the discharge, limiting the ability of the operator to respond proactively.

#### **4.3.3 Deep Dielectric Charging**

Many authors have made the point that, in addition to surface charging, deep dielectric charging due to more energetic electrons can cause discharges and can cause spacecraft anomalies.

- Adamo [1983] notes that, of all the transient pulses recorded in the first two years of the SCATHA mission, the only one that was associated with a spacecraft anomaly occurred with no surface charging recorded by the surface potential monitors, and no enhanced flux of electrons in the tens of keV range, but with a sustained high flux of relativistic electrons, with energy above 1 MeV.
- Koons [1983] noted that many discharges were observed in the absence of surface charging, as recorded by the surface potential monitors, but that many of these followed a sustained high flux of electrons above 300 keV.
- Koons [1991] noted that internal discharges typically occurred when the flux of electrons in the several hundred keV range was high and the flux of electrons in the tens of keV range was low. Since the latter electrons cause surface charging, the internal discharges are not associated with surface potential monitor measurements.
- Vampola [1987] observed that many operational anomalies on the Defense Support Program geosynchronous spacecraft coincided with a sustained high flux of electrons with energy above 1.2 MeV.

- Gussenhoven [1996] showed that the charging that creates most operational anomalies is induced by high energy electrons, with energies from a few hundred keV to a few MeV, and are not associated with surface charging.
- Frederickson [1996] showed that, on the CRRES spacecraft, the rate of discharges in internal dielectrics was proportional to the flux of high energy electrons. He also makes the point that, to determine if electrostatic discharges are occurring on a specific spacecraft, radiation detectors are needed.

We at Amptek have concluded that deep dielectric charging is as much of a hazard as surface charging, and that prior warning can be obtained by summing the flux over a time period of many hours. The data clearly show that measurements of the environment provide the best advance warning for dielectric charging that causes operational anomalies.

## 5 SPACECRAFT SPECIFIC DESIGN, FABRICATION, AND TEST

A key part of this CEASE Support Contract was carrying out the spacecraft specific tasks required to integrate the instruments on actual spacecraft. The S/N 001 instrument was designated for flight on the Space Test Research Vehicle 1c (STRV-1c) spacecraft and S/N 002 on the Tri-Service Experiment 5 (TSX-5) spacecraft. Spacecraft specific tasks included (1) designing and fabricating certain spacecraft specific hardware components, related to the spacecraft interface, (2) implementing flight software for the particular interfaces, (3) writing GSE software to interface with the flight software and hardware, (4) carrying out the necessary environmental tests, and (4) supporting delivery, integration, and launch.

### 5.1 SPACECRAFT SPECIFIC HARDWARE

The standard CEASE serial command and telemetry interface is an asynchronous serial RS422 interface. This interface is used in bench testing of the instrument and is available on all CEASE units. The STRV-1c spacecraft has a custom serial, with optical isolation, while the TSX-5 spacecraft has a MILSTD-1553B interface. Therefore, each instrument required a custom I/O board to support these interfaces. S/N 001 required a custom FPGA to implement the interface, while for S/N 002 a commercially available 1553B chipset was used. Both spacecraft use standard, 28V power buses with typical specifications, so the standard power supply was used for both.

### 5.2 FLIGHT SOFTWARE

Flight software was written to implement (1) the engineering algorithms discussed in Section 4.1, (2) to format the results into the standard telemetry packets, and (3) to interface with the spacecraft.

The three types of telemetry that are available were discussed in Section 2.1.4. Detailed information is available in the *CEASE Data Processing Document*, Amptek document CES-770-A0.DOC. CEASE provides three different telemetry types. The Science Data packet contains raw count values directly from the CEASE Sensors. It is a 56 byte packet, updated every 5 seconds on S/N 002 and every 10 second on S/N 001. The Engineering Data Packet contains fully processed data, the results of the status register algorithms. It is a 10 byte packet, updated every 60 seconds. The History Data Packet contains summaries of the environment, a mix of raw and processed data. History data are placed into a circular buffer every 15 minutes, with a 72 hour buffer depth. All three data packets are always available to the spacecraft.

Table 8. Engineering Data Packet

Byte #	Meaning
0	Synch Byte
1	WF status since CRF Reset command. Each bit corresponds to one of the eight Warning Flags (Table 3). This byte shows which WF were tripped since a Reset command was sent.
2	Current WF status. Each bit corresponds to one of the eight Warning Flags (Table 3). This byte shows which WF were tripped in the previous 60 seconds.
3	SR <sub>1</sub> and SR <sub>2</sub> . See Table 2 and Table 7. Each status register is 4 bits (1 nibble)
4	SR <sub>3</sub> and SR <sub>4</sub>
5	SR <sub>5</sub> and SR <sub>6</sub>
6	SR <sub>7</sub> and SR <sub>8</sub>
7	CEASE Status
8	Checksum byte 1
9	Checksum byte 2

### 5.3 GSE SOFTWARE

The Flight Display GSE software was designed to facilitate functional testing, calibration, integration with the spacecraft, and on-orbit operations. To support the various operational schemes for CEASE, the Flight Display GSE software processes and displays all types of CEASE data. A configuration file is used to tailor the displays to specific CEASE instruments.

CEASE telemetry must be processed by mission-specific software that correctly formats the CEASE telemetry for this Flight Display GSE software. The required format is a file with records each containing 70 bytes. Bytes 0-3 contain a time stamp. Bytes 4-5 contain the packet (i.e. record) ID. This ID is: 0 for Engineering, 1 for Science, and 2 for History. Bytes 6-69 contain the data:

- Engineering      10 bytes of data & 54 bytes of zero-fill
- Science            56 bytes of data and 8 bytes of zero-fill
- History            52 bytes of data and 12 bytes of zero-fill

Data files can be viewed real-time or in playback. In Figure 5, the playback controls are shown in the lower right corner of the display. Alternatively, file control is available from the *Control* pulldown menu. The Flight Display GSE can also be used to process the CEASE data into individual files containing comma separated variables. This feature can be used to import CEASE data into other software for further analysis.

The software logs the receipt of all types of CEASE data, including commands issued to the instrument. The tracking functions are displayed on the Logs, Records, and Telemetry pages. Only data with proper sync and checksums are displayed by the Flight Display GSE on the Science, Engineering and History pages. Rejected data from the formatted file are displayed in an Error box on the Records page. The filename, record number, CEASE frame counter and time stamps are visible from any page. Accumulation time, if accumulate is invoked, is also always displayed.

The Warning Flags are always available to the user. The box is green if the flag has not been set. If the flag has been set, the box initially is blue with a white X in it. If the next frame still has the bit set, then the box becomes red with a white X through it. This scheme was chosen to handle the case where telemetry signals could be noisy, with bits inadvertently set in transmission rather than by CEASE.

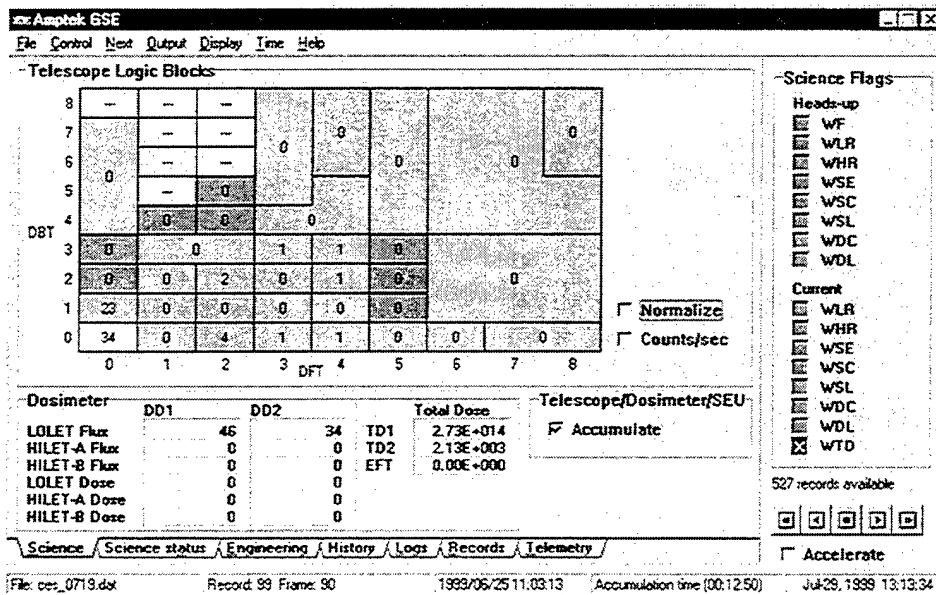


Figure 5. Flight GSE Science Display Page

#### Telescope Data

The data collected from the CEASE telescope are stored in 80 channels, corresponding to different energy deposition values in the front (DFT) and back (DBT) telescope detectors. Each detector has eight energy deposition thresholds set in the readout electronics with thresholds TFA through TFH for DFT, and

TBA through TBH for DBT. The thresholds separate the range of the possible energy depositions by incident particles into 80 regions called Logic Boxes (LB) Selected LBs are contained in the CEASE Science Data Packet.

The critical LBs are updated at the rate of the Science Data Interval. LBs that are used primarily for noise checks are subcommutated in the telemetry and their update rate is once per 32 major frames. Those boxes are outlined in the telescope portion of the display on the Science Page.

On this page, the boxes are color coded for update rate - blue for SDI update rate and green for subcommutated data. The value in yellow box in the lower left corner is the sum of the telescope counts updated at the SDI rate. This value is not part of the downlinked telemetry, but is calculated by the GSE software. The user has the option to view the counts in the LBs normalized to this calculated total. Also, the data can be displayed as a count rate, by selecting the counts per second option. *Normalize* and *Counts/sec* only apply to telescope data. *Accumulate* applies to the Telescope total, to the LBs updated at the SDI rate, and to the SEE counts.

The particle telescope data are also used to determine the surface dose to unshielded components. The critical parameter is the Effective 1 MeV fluence. This value is displayed in the *EFT* box. This value is in the 32-deep subcommutated channel in the Science packet and is updated only when all four bytes are received.

#### Dosimeter Data

The DD1 and DD2 LOLET and HILET fluxes and doses displayed by the Flight GSE software correspond to the energy ranges in the flight instrument. These data are duty cycle corrected in the Flight GSE processing. The data displayed are in counts, not rads. The flux and dose values can be Accumulated. Total Doses from DD1 and DD2 are displayed in TD1 and TD2, respectively. These are included in the 32-deep subcommutated channel in the Science packet and are updated accordingly. These total dose values are not affected when *Accumulate* is selected.

#### SEE Data

The SEE data are available on the Science Status page. There is also a low level threshold setting that is ~1 MeV and is used to calibrate the SEU detector. The ~50 MeV threshold is the NORMAL threshold and the ~1 MeV threshold is the LOW threshold. The threshold status is displayed on the GSE.

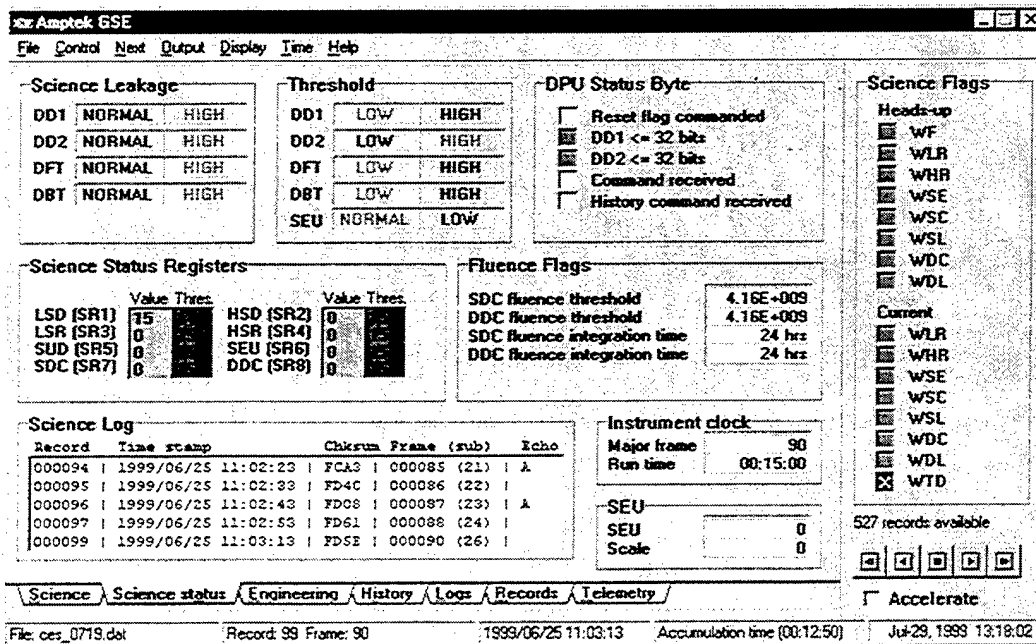


Figure 6. Flight GSE Science Status Page

Instrument housekeeping and status are maintained on the Science Status Page. The detector leakage current monitors and hardware thresholds are displayed. Command receipt and processing, detected

dosimeter noise, and watchdog timer resets are viewed in the *DPU Status Byte* section. The Hazard Register and the Warning Flag register thresholds are in the *Science Status Registers Value and Thres.* section. Instrument frame counter and time since power-on are shown in the *Instrument Clock* area.

#### **5.4 ENVIRONMENTAL TESTING**

Prior to delivery, the CEASE instruments underwent the typical battery of environmental tests, including thermal vacuum, shake and vibration, and electromagnetic cleanliness/electromagnetic interference.

Thermal vacuum cycling generally included 5 thermal cycles, ranging from -20°C to +50°C, while under vacuum. These tests were conducted with a stimulus source cover on the instrument. A Comprehensive Performance Test was executed at the beginning and end of the thermal cycling at room temperature and at each temperature limit for each of the thermal cycles. The data were examined for significant drift in performance and for failure of CEASE to execute commands. Additionally, Hot starts were performed at the specified spacecraft power bus extremes. Random vibration testing following final staking and cleaning of the instruments. The instrument were not powered during the test. EMI/EMC Tests were based upon MIL-STD-461(c), tailored for the requirements of each spacecraft. Tests were conducted at a certified EMI/EMC testing facility, with Amptek personnel monitoring CEASE performance throughout both emissions and susceptibility testing.

#### **5.5 INTEGRATION AND LAUNCH SUPPORT ACTIVITIES**

Delivery of CEASE S/N 001 to the British Defense Evaluation and Research Agency (DERA) UK for integration onto STRV-1c was accomplished in February 1999. Final testing was conducted per the DERA Experiment Acceptance Test Plan (EATP) verifying that CEASE meets the mechanical, functional, power, OBDH, and magnetic susceptibility requirements. An Acceptance Data Package, meeting the requirements of the EATP, was completed and delivered with the instrument. The STRV-1c spacecraft was successfully launched on 15 Nov 2000. CEASE initial turn-on and checkout was successfully accomplished on 27 Nov 2000.

CEASE S/N 002 was delivered to Orbital Sciences Corporation in June 1998 for integration onto the TSX-5 spacecraft. S/N 002 was successfully mechanically and electrically integrated with the TSX-5 spacecraft. The TSX-5 spacecraft was successfully launched on 7 June 2000. CEASE initial turn-on and checkout was successfully accomplished on 8 June 2000. The TSX-5 orbit, 410 x 1710 km with an inclination of 70°, is a very interesting orbit for CEASE, since apogee occurs in the radiation belts, in a very hazardous environment, perigee occurs in a very benign environment, and the high inclination portions of the trajectory pass through the auroral oval and the horns of the outer belts, a highly variable environment.

Amptek personnel supported the integration and launch of these instruments in a variety of ways, from traveling to contractor facilities to carry out deliveries and tests, to writing test procedures and other documentation, to evaluating test data. Preliminary analysis has indicated that the instruments are operating properly.



### References

- R.C. Adamo, J.R. Matarese, "Transient Pulse Monitor Data from the P78-2 (SCATHA) Spacecraft," *J. Spacecraft and Rockets*, Vol 20, No. 5, p 432 (1983)
- A.R. Frederickson, "Upsets Related to Spacecraft Charging," *IEEE Trans. Nucl. Sci.*, Vol. 43, No. 2, p 426 (1996)
- H.B. Garret, "The Charging of Spacecraft Surfaces," *Rev. Geophys. & Space Phys.*, Vol 19, No. 4, p 577 (1981)
- M.S. Gussenhoven, E.G. Mullen, D.H. Brautigam, "Improved Understanding of the Earth's Radiation Belts from the CRRES Satellite," *IEEE Trans. Nucl. Sci.*, Vol. 43, No. 2, p 353 (1996)
- H.C. Koons, "Summary of Environmentally Induced Discharges on the P78-2 (SCATHA) Satellite," *J. Spacecraft and Rockets*, Vol 20, No. 5, p 425 (1983)
- H.C. Koons, D.J. Gorney, "Relationship Between Electrostatic Discharges on Spacecraft P78-2 and the Electron Environment," *J. Spacecraft and Rockets*, Vol 28, No. 6, p 683 (1991)
- H.C. Koons, P.F. Mizera, J.L. Roeder, J.F. Fennell, "Severe Spacecraft Charging Event on SCATHA in September 1982," *J. Spacecraft and Rockets*, Vol 25, No. 3, p 239 (1988)
- P.F. Mizera, "A Summary of Spacecraft Charging Results," *J. Spacecraft and Rockets*, Vol 20, No. 5, p 438 (1983)
- E.G. Mullen, M.S. Gussenhoven, D.A. Hardy, T.A. Aggson, "SCATHA Survey of High Level Spacecraft Charging in Sunlight," *J. Geophys. Res.*, Vol 91, No. A2, p 1474 (1986)
- A. Vampola, *J. Electrostatics*, Vol 20, No. 1, p 21 (1987)